Least Squares Based PID Control of an Electromagnetic Suspension System

Yon-Mook Park* and Min-Jea Tahk**

Division of Aerospace Engineering
Department of Mechanical Engineering
Korea Advanced Institute of Science and Technology
373-1 Guseong-dong, Yuseong-gu, Daejeon 305-701, Republic of Korea

Myeong-Ryong Nam***, In-Ho Seo**** and Sang-Hyun Lee****

Satellite Technology Research Center
Korea Advanced Institute of Science and Technology
373-1 Guseong-dong, Yuseong-gu, Daejeon 305-701, Republic of Korea

Jong-Tae Lim*****

Division of Electrical Engineering
Department of Electrical Engineering & Computer Science
Korea Advanced Institute of Science and Technology
373-1 Guseong-dong, Yuseong-gu, Daejeon 305-701, Republic of Korea

Abstract

In this paper, we develop the so-called functional test model for magnetic bearing wheels. The functional test model developed in this paper is a kind of electromagnetic suspension systems and has three degree of freedom, which consists of one axial suspension from gravity and the other two axes gimbaling capability to small angle, and does not include the motor. For the control of the functional test model, we derive the optimal electromagnetic forces based on the least squares method, and use the proportional-integral -derivative controller. Then, we develop a hardware setup, which mainly consists of the digital signal processor and the 12-bit analog-to-digital and digital-to-analog converters, and show the experimental results.

Key Word : Electromagnetic suspension system, Magnetic bearing wheel, Least squares method, Proportional-integral-derivative control

Introduction

In general, spacecraft in orbit is equipped with reaction or momentum wheels serving as actuators in the attitude control system. Until now, ball bearing wheels have been dominantly used in that application. However, among the various kinds of onboard system components, ball bearing wheels have been identified as one of the main sources of vibration noise due to the wear as a result of mechanical contact of rotor and stator, residual unbalances, and bearing imperfections[1].

* Graduate Student
   E-mail : ympark@fdcl.kaist.ac.kr,   TEL : 042-869-8610,   FAX : 042-861-0064
** Professor
*** Research Professor
**** Researcher
***** Professor

These disadvantages can be avoided by using magnetic bearing wheels. Compared with ball bearing wheels, magnetic bearing wheels can suspend a rotor by use of the magnetic or electromagnetic force, by which the high rotational speed of rotor, no contact, and no lubrication can be possible. Moreover, if the wheel provides a vernier gimbaling capability, the three-axis attitude control can be possible with only a single wheel [2]. Magnetic bearing wheels should be ideally suited to exhibit very low noise figures since they have no mechanical contact between stator and rotor. However, there are several sources of disturbing forces in magnetic bearing wheels. Some of these sources come from an unfavorable design, and some others are of principle nature but can be overcome by adopting various kinds of control means (e.g. [3]-[10]).

In this paper, we develop the so-called functional test model (FTM) in order to obtain the basic electromagnetic suspension technique of magnetic bearing wheels. In the FTM, the active control of three degree of freedom (DOF), which consists of one axial suspension from gravity and the other two axes gimbaling capability to small angle, is possible but the motor is not included.

For the control of the FTM, we utilize the least squares method in order to optimize the electromagnetic forces, and employ the proportional-integral-derivative (PID) controller. Especially, we develop a hardware setup using the digital signal processor, and show the experimental results for the FTM.

This paper is organized as follows. First, we give the mathematical modeling of the FTM. Also, based on the least squares method, we derive the optimal electromagnetic forces of the FTM. Next, we describe the mechanical structure of the FTM as well as the electronics for the FTM. Then, we use the PID controller for the control of the FTM, and give the experimental results. Finally, we summarize the conclusion of the paper.

Modeling of the Functional Test Model

Dynamics

Fig. 1 shows the schematic diagram of the functional test model (FTM) for magnetic bearing wheels developed in this paper, where $S_1 - S_4$ are four gap sensors and $E_1 - E_4$ are four pairs of electromagnets.

The FTM has three degree of freedom (DOF) which consists of the Z axis suspension from gravity and the X and Y axes gimbaling capability to small angle. Then, the dynamics of the FTM become

$$m\ddot{z} = f_z, \quad I\ddot{\phi} = T_x, \quad I\ddot{\theta} = T_y. \quad (1)$$

where m is the mass of the rotor, I is the inertia of the rotor for the X and Y axes, z is the axial displacement of the rotor, ϕ is the rotational angle of the X axis, θ is the rotational angle of the Y axis. Moreover, f_z is the electromagnetic force of the Z axis, and T_x and T_y are the torques of the X and Y axes, respectively.

If we consider four electromagnets $E_1 - E_4$ shown in Fig. 1, the f_z, T_x, and T_y of Eq. (1) can be represented by
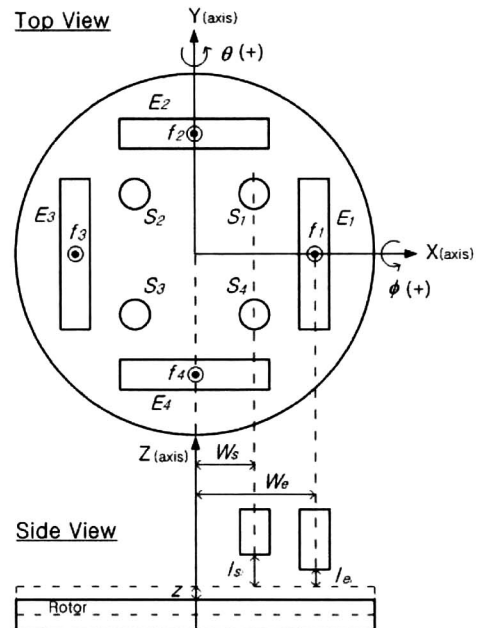

Fig. 1. Schematic diagram of the functional test model

$$\begin{aligned}
f_z &= f_1 + f_2 + f_3 + f_4 - mg, \\
T_x &= W_e(f_2 - f_4), \\
T_y &= W_e(f_3 - f_1),
\end{aligned} \tag{2}$$

respectively, where f_i, $i = 1, \cdots, 4$ are the electromagnetic forces of each electromagnet, W_e is the length from the center of the rotor to the electromagnet, g is the acceleration of gravity.

Kinematics

Under the assumption that the angle displacements of the rotor are very small, the gap sensor measurement from the ith gap sensor to the rotor, denoted by l_{s_i}, are given as follows.

$$\begin{aligned}
l_{s_1} &= L_{s_1} + \delta L_{s_1} \cong L_{s_1} - z + W_s\theta - W_s\phi, \\
l_{s_2} &= L_{s_2} + \delta L_{s_2} \cong L_{s_2} - z - W_s\theta - W_s\phi, \\
l_{s_3} &= L_{s_3} + \delta L_{s_3} \cong L_{s_3} - z - W_s\theta + W_s\phi, \\
l_{s_4} &= L_{s_4} + \delta L_{s_4} \cong L_{s_4} - z + W_s\theta + W_s\phi,
\end{aligned} \tag{3}$$

where L_{s_i}, $i = 1, \cdots, 4$ are the displacements from each gap sensor to the rotor at the equilibrium state, δL_{s_i}, $i = 1, \cdots, 4$ are the perturbation terms of each L_{s_i}, and W_s is the length from the center of the rotor to the gap sensor.

Then, from Eq. (3), the z, ϕ, and θ can be calculated as follows.

$$z = \frac{1}{4}[(L_{s_1} + L_{s_2} + L_{s_3} + L_{s_4}) - (l_{s_1} + l_{s_2} + l_{s_3} + l_{s_4})], \tag{4}$$

$$\phi = \frac{1}{4W_s}[(l_{s_3} + l_{s_4} - l_{s_1} - l_{s_2}) - (L_{s_3} + L_{s_4} - L_{s_1} - L_{s_2})], \tag{5}$$

$$\theta = \frac{1}{4W_s}[(l_{s_1} + l_{s_4} - l_{s_2} - l_{s_3}) - (L_{s_1} + L_{s_4} - L_{s_2} - L_{s_3})]. \tag{6}$$

Also, the displacement from the ith electromagnet to the rotor, denoted by l_{e_i}, are given by

$$\begin{aligned}
l_{e_1} &= L_{e_1} + \delta L_{e_1} \cong L_{e_1} - z + W_e\theta, \\
l_{e_2} &= L_{e_2} + \delta L_{e_2} \cong L_{e_2} - z - W_e\phi, \\
l_{e_3} &= L_{e_3} + \delta L_{e_3} \cong L_{e_3} - z - W_e\theta, \\
l_{e_4} &= L_{e_4} + \delta L_{e_4} \cong L_{e_4} - z + W_e\phi,
\end{aligned} \tag{7}$$

where L_{e_i}, $i = 1, \cdots, 4$ are the displacements from each electromagnet to the rotor at the equilibrium state, δL_{e_i}, $i = 1, \cdots, 4$ are the perturbation terms of each L_{e_i}.

Electromagnetic Forces

Note that Eq. (2) can be written by

$$Af = b, \tag{8}$$

where

$$A = \begin{bmatrix} 1 & 1 & 1 & 1 \\ 0 & W_e & 0 & -W_e \\ -W_e & 0 & W_e & 0 \end{bmatrix}, \quad b = \begin{bmatrix} f_z + mg \\ T_x \\ T_y \end{bmatrix}, \quad f = \begin{bmatrix} f_1 \\ f_2 \\ f_3 \\ f_4 \end{bmatrix}. \tag{9}$$

As shown in Eq. (8), after designing the three control inputs of f_z, T_x, and T_y, we must determine the four electromagnetic forces f_i, $i = 1, \cdots, 4$ in order to apply the designed control inputs to the FTM. In this case, Eq. (8) has infinitely many solutions for the four electromagnetic forces since it is under-determined with three equations in four unknowns f_i, $i = 1, \cdots, 4$.

Among many solutions to the above problem, we take a meaningful thing by considering the least squares problem. Before giving a meaningful solution, we define the singular value decomposition.

Definition 1 [11]: Let $A \in R^{m \times n}$ have the rank of $r < n$. Then, the singular value decomposition of A is given by

$$
\begin{aligned}
U \Sigma V^T &= [\, U_1 \quad U_2 \,]
\begin{bmatrix}
\Sigma_1 & 0_{\, r \times (n-r)} \\
0_{\,(m-r) \times r} & 0_{\,(m-r) \times (n-r)}
\end{bmatrix}
\begin{bmatrix}
V_1^T \\
V_2^T
\end{bmatrix} \\
&= U_1 \Sigma_1 V_1^T ,
\end{aligned}
\tag{10}
$$

where $U \triangleq [\, U_1 \quad U_2 \,] \in R^{m \times m}$ and $V \triangleq [\, V_1 \quad V_2 \,] \in R^{n \times n}$ are orthogonal matrices with $U_1 \in R^{m \times r}$, $U_2 \in R^{m \times (m-r)}$, $V_1 \in R^{n \times r}$, and $V_2 \in R^{n \times (n-r)}$. Moreover, $\Sigma_1 \in R^{r \times r}$ is a diagonal matrix given by

$$
\Sigma_1 =
\begin{bmatrix}
\sigma_1 & 0 & 0 & \cdots & 0 \\
0 & \sigma_2 & 0 & \cdots & 0 \\
0 & 0 & \sigma_3 & \cdots & 0 \\
\vdots & \vdots & \vdots & \ddots & \vdots \\
0 & 0 & 0 & \cdots & \sigma_r
\end{bmatrix}
\tag{11}
$$

with the entries satisfying

$$
\sigma_1 \geq \sigma_2 \geq \ldots \geq \sigma_r > 0,
\tag{12}
$$

and $0_{\, a \times b}$ denotes the $a \times b$ zero matrix. ∎

Then, we show that the singular value decomposition provides the key to solve the least squares problem for design of the optimal electromagnetic forces.

Theorem 1: For Eq. (8), let the singular value decomposition of A be $U \Sigma V^T$ and define

$$
A^+ \triangleq V \Sigma^+ U^T,
$$

where A^+ denotes the pseudo-inverse of A. Then, the following electromagnetic force vector

$$
\begin{aligned}
f = A^+ b &= V \Sigma^+ U^T b \\
&=
\begin{bmatrix}
\dfrac{1}{4}(f_z + mg) - \dfrac{1}{2}\dfrac{T_y}{W_e} \\[4pt]
\dfrac{1}{4}(f_z + mg) + \dfrac{1}{2}\dfrac{T_x}{W_e} \\[4pt]
\dfrac{1}{4}(f_z + mg) + \dfrac{1}{2}\dfrac{T_y}{W_e} \\[4pt]
\dfrac{1}{4}(f_z + mg) - \dfrac{1}{2}\dfrac{T_x}{W_e}
\end{bmatrix}
\triangleq
\begin{bmatrix}
f_1 \\ f_2 \\ f_3 \\ f_4
\end{bmatrix}
\end{aligned}
\tag{13}
$$

is a solution of Eq. (8). Moreover, if h is any other solution of Eq. (8), then

$$\|h\|_2 > \|f\|_2 . \tag{14}$$

Proof: First, let $f \in R^4$ and define

$$c \triangleq U^T b = \begin{bmatrix} c_1 \\ c_2 \end{bmatrix} , \qquad d \triangleq V^T f = \begin{bmatrix} d_1 \\ d_2 \end{bmatrix} , \tag{15}$$

where $c_1 \in R^3$ and $d_1 \in R^3$. From Definition 1 and Eq. (15), we can obtain

$$
\begin{aligned}
\|b - Af\|_2^2 &= \|U^T\|_2^2 \|b - Af\|_2^2 \\
&= \|U^T b - U^T (U \Sigma V^T f)\|_2^2 \\
&= \|U^T b - \Sigma V^T f\|_2^2 \\
&= \|c - \Sigma d\|_2^2 \\
&= \left\| \begin{bmatrix} c_1 \\ c_2 \end{bmatrix} - \begin{bmatrix} \Sigma_1 & 0 \\ 0 & 0 \end{bmatrix} \begin{bmatrix} d_1 \\ d_2 \end{bmatrix} \right\|_2^2 \\
&= \left\| \begin{bmatrix} c_1 - \Sigma_1 d_1 \\ c_2 \end{bmatrix} \right\|_2^2 \\
&= \|c_1 - \Sigma_1 d_1\|_2^2 + \|c_2\|_2^2 ,
\end{aligned}
\tag{16}
$$

where $\| \cdot \|_2$ denotes the Euclidean norm. Since c_2 is independent of f, it follows that $\|b - Af\|_2^2$ will be minimal if and only if

$$\|c_1 - \Sigma_1 d_1\|_2 = 0 . \tag{17}$$

Furthermore, $\|b - Af\|_2^2$ will be zero if and only if

$$\|c_1 - \Sigma_1 d_1\|_2 = 0 , \quad c_2 = 0 . \tag{18}$$

Thus, f becomes a solution to Eq. (8) if and only if $f = Vd$ and $c_2 = 0$, where

$$d = \begin{bmatrix} d_1 \\ d_2 \end{bmatrix} = \begin{bmatrix} \Sigma_1^{-1} c_1 \\ d_2 \end{bmatrix} . \tag{19}$$

Especially, $f = A^+ b$ is a solution to Eq. (8) since

$$
\begin{aligned}
f &= Vd = V \begin{bmatrix} \Sigma_1^{-1} c_1 \\ 0 \end{bmatrix} \\
&= V \begin{bmatrix} \Sigma_1^{-1} & 0 \\ 0 & 0 \end{bmatrix} \begin{bmatrix} c_1 \\ c_2 \end{bmatrix} \\
&= V \Sigma^+ c = V \Sigma^+ U^T b = A^+ b \\
&= \begin{bmatrix}
\frac{1}{4}(f_z + mg) - \frac{1}{2}\frac{T_y}{W_e} \\
\frac{1}{4}(f_z + mg) + \frac{1}{2}\frac{T_x}{W_e} \\
\frac{1}{4}(f_z + mg) + \frac{1}{2}\frac{T_y}{W_e} \\
\frac{1}{4}(f_z + mg) - \frac{1}{2}\frac{T_x}{W_e}
\end{bmatrix} .
\end{aligned}
\tag{20}
$$

Next, if h is any other solution to Eq. (8), h must be of the form

$$h = Vd = V\begin{bmatrix} \Sigma_1^{-1} c_1 \\ d_2 \end{bmatrix}, \tag{21}$$

where $d_2 \neq 0$. Then, for h of Eq. (21), we can obtain

$$\begin{aligned} \|h\|_2^2 &= \|Vd\|_2^2 = \|d\|_2^2 \\ &= \|\Sigma_1^{-1} c_1\|_2^2 + \|d_2\|_2^2 \\ &> \|\Sigma_1^{-1} c_1\|_2^2 = \|f\|_2^2. \end{aligned} \tag{22}$$

This completes the proof.   ■

Remark 1: Note that the electromagnetic force vector f given in Eq. (13) is obtained by utilizing the least squares method. Therefore, as shown in Theorem 1, the solution f of Eq. (13) becomes the minimal norm solution to Eq. (8) such that the condition of (14) holds for any other solution h to Eq. (8).

In practice, the electromagnetic forces given in Eq. (13) are made by currents. Thus, we must generate currents in the coils which wind each electromagnet. By applying the Maxwell's equation to the electromagnet of the FTM, we can obtain the following equation for the coil currents of each electromagnet:

$$i_i = \frac{l_{e_i}}{n} \sqrt{\frac{8 f_i}{\mu_0 G}}, \quad i = 1, \cdots, 4, \tag{23}$$

where i_i is the coil current of the ith electromagnet, n is the number of coil turns, μ_0 is the magnetic permeability in the air, G is the cross area of the electromagnet, and l_{e_i} and f_i are given in Eqs. (7) and (13), respectively.

Mechanical Structure and Control Electronics

Mechanical Structure

Based on the requirements of the reaction wheel in small satellites such as the Korea Institute of Technology Satellite (KITSAT)-1, 2, 3, and the Science and Technology Satellite (STSAT)-1 which have been developed by the Satellite Technology Research Center (SaTReC) in Korea, the major mechanical specifications of the FTM is described in Table 1. Since the motor is not included in design of the FTM, the specification about the motor is excluded.

Table 1. Mechanical Specifications of the Functional Test Model.

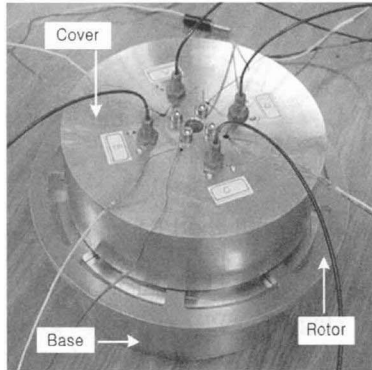| Item	Value	Unit
Active control axis	3	DOF
Dimension	φ 140 × 100	mm
Mass of rotor	1	kg
Nominal gap	0.8	mm
Gimbaling angle	+/- 0.12	deg
Gap sensor	4	number
Electromagnet	4	pair
Number of coil turn	240	turn

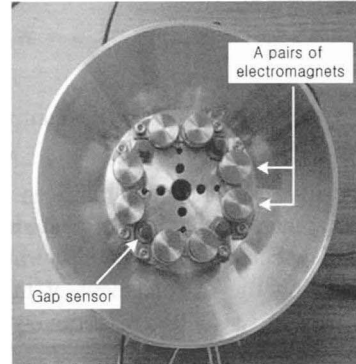Fig. 2. Perspective view of the functional test model.

Fig. 3. Four pairs of electromagnets and four gap sensors of the functional test model.

Then, Fig. 2 shows the perspective view of the FTM, in which the base and cover are equivalent to the stator and they support the rotor. Next, Fig. 3 shows the four pairs of electromagnets as well as the four gap sensors, which are attached on the lower surface of the cover in order to generate the electromagnetic forces and measure the suspension displacement of the rotor, respectively. Note that the AEC-5505 model of eddy current-typed gap sensor from Applied Electronics Co., Ltd. is used in the FTM.

Also, Fig. 4 shows the electromagnetic field analysis of the SUS 410 ferromagnetic material, made by stainless steel, used in the FTM. In Fig. 4, the

Fig. 4. Electromagnetic field analysis of the functional test model.

electromagnetic field is formed closely around the electromagnet. Therefore, the interference of the electromagnetic field between the neighboring electromagnets is very small, which is a desirable phenomenon for the control of the electromagnetic force of each electromagnet.
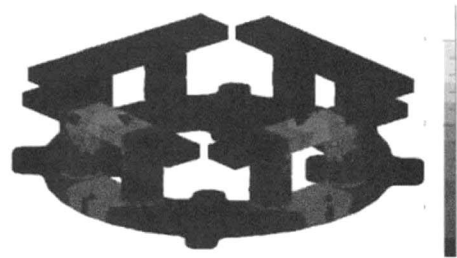
Control Electronics

For the electronic control of the FTM, we develop an control electronics which mainly consists of the 32-bit floating-point digital signal processor (DSP) of TMS320C32 from Texas Instruments, the 12-bit analog-to-digital converter (ADC), and the digital-to-analog converter (DAC). Note that the DSP is used for fast calculation, and the 12-bit ADC and DAC are used to read the output from the gap sensor and to make the electromagnetic forces, respectively.

Also, we develop a power module for the current control of the FTM, which converts the output voltage of the DAC to a suitable current and transmits the current into the coil of the electromagnet. The power module is linear-typed, and the maximum output current can be adjustable.

Experimental Results

Control Scheme

In order to control the three DOFs of magnetic levitation of the FTM, we use a proportional-integral-derivative (PID) controller since it is easy to implement with a practical usefulness.

The PID controller for the FTM takes the following form:

$$u = K_P e + K_D \frac{de}{dt} + K_I \int_0^t e(\tau)\,d\tau, \qquad (24)$$

where $u \triangleq [f_z \ T_x \ T_y]^T$ is the control inputs of the FTM, $e \triangleq x_{ref} - x$ is the error between $x \triangleq [z \ \phi \ \theta]^T$ and its reference x_{ref}. Moreover, $K_P = K_P^T > 0$, $K_I = K_I^T > 0$, $K_D = K_D^T > 0$ are the 3×3 positive definite gain matrices of the PID controller.

Fig. 5 shows the control system configuration of the FTM with the PID controller given by Eq. (24). The control system configuration consists of the four stages. Specifically, in the first stage, after detecting the displacement of the rotor from each gap sensor, we calculate the z, ϕ, and θ given by Eqs. (4)-(6), respectively. Next, in the second stage, the PID controller given by Eq. (24) produces the f_z, T_x, and T_y. Then, in the third stage, we obtain the four electromagnetic forces f_i, $i = 1,\cdots,4$ by Eq. (13). Finally, in the fourth state, we calculate the control currents of the electromagnets by Eq. (23).
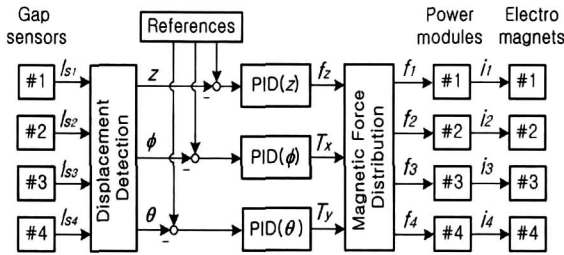

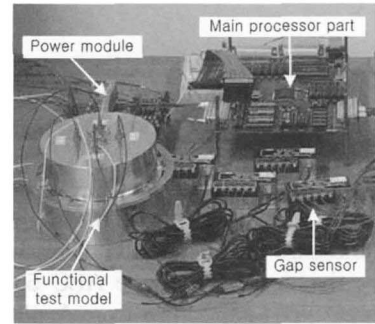Fig. 5. Control system configuration of the functional test model.

Fig. 6. Hardware setup for the functional test model.

Experiment and Analysis

Fig. 6 shows the hardware setup for the FTM developed in this paper. With this setup, we obtain experimental results.

The control objective is to levitate the rotor at 0.3 mm from the base of the FTM, and regulate the ϕ and θ to zeros. Thus, the x_{ref} is set to be $x_{ref} = [z_{ref} \ \phi_{ref} \ \theta_{ref}]^T = [0.3 \text{ mm } 0 \text{ deg } 0 \text{ deg}]^T$. Note that the control algorithm is implemented by C language with a sampling rate of 0.001 sec.

Among some candidates of the PID control gains which can provide the PID controller achieving the control objective, the following gains are chosen in the experiment.

$$\begin{aligned} K_P &= \text{diag}\,[1000,\ 20,\ 20], \\ K_I &= \text{diag}\,[5000,\ 8.33,\ 8.33], \\ K_D &= \text{diag}\,[100,\ 0.013,\ 0.013], \end{aligned} \qquad (25)$$

where diag implies the diagonal matrix.

Then, the responses of the FTM and the control currents obtained by the experiment are shown in Figs. 7 and 8, respectively. As shown in Figs. 7 and 8, the PID controller stabilizes the state of the FTM. Moreover, against the external disturbances imposed by a hand at about 20 seconds, the recovery time of the state response to the reference command is somewhat fast. Also, the magnitudes of each control current are admissible. Note that the state histories obtained in the experiment show very high frequency noises since the design considered in this paper does not include a filter. Thus, future work may include a filter design which can provide a good quality of the measurement. Also,
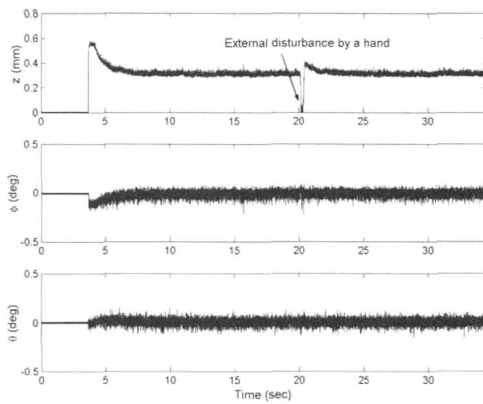
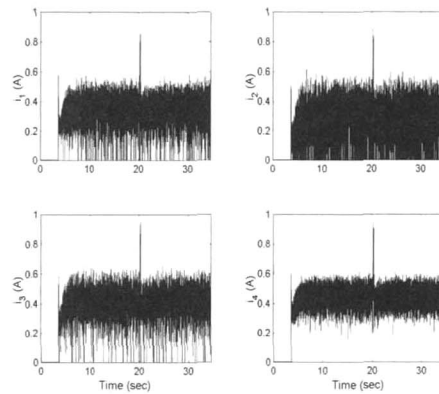Fig. 7. Responses of the functional test model.

Fig. 8. Control currents of the functional test model.

based on the technology developed in this paper, the development of the active magnetic bearing system with an active vibration suppression (e.g. [12] and [13]) will be proceed.

Conclusions

In this paper, we have developed an electromagnetic suspension system for magnetic bearing wheels. For the control of the electromagnetic suspension system, the proportional-integral-derivative controller has been used based on the least squares method. Then, we have developed a hardware setup, which mainly consists of the digital signal processor and 12-bit analog-to-digital and digital-to-analog converters, and obtain the satisfactory experimental results.

Acknowledgement

References

1. Bichler, U. J., "A double gimbaled magnetic bearing momentum wheel for high pointing accuracy and vibration sensitive space applications," *Proceedings of the 1st ESA Int. Conf. on Spacecraft Guidance, Navigation and Contr. Syst*, Noordwijk, Netherlands, June, 1991, pp. 393-398.

2. Horiuchi, Y., Inoue, M., Sato, N., Hashimoto, T., and Ninomiya, K., "Development of magnetic bearing momentum wheel for ultra-precision spacecraft attitude control," *Proceedings of the 7th Int. Symp. on Magn. Bearings*, Zurich, Switzerland, Aug., 2000, pp. 525-530.

3. Matsumura, F., Namerikawa, T., Hagiwara, K., and Fujita, M., "Application of gain scheduled H_∞ robust controllers to a magnetic bearing," *IEEE Trans. Contr. Syst. Technol.*, Vol. 4, No. 5, 1996, pp. 484-493.

4. Nonami, K., and Ito, T., "μ synthesis of flexible rotor-magnetic bearing systems," *IEEE Trans. Contr. Syst. Technol.*, Vol. 4, No. 5, 1996, pp. 503-512.

5. De Queiroz, M. S., and Dawson, D. M., "Nonlinear control of active magnetic bearings: A backstepping approach," *IEEE Trans. Contr. Syst. Technol.*, Vol. 4, No. 5, 1996, pp. 545-552.

6. Nam, M.-R., Hashimoto, T., and Ninomiya, K., "Design of H_∞ attitude controllers for spacecraft

using a magnetically suspended momentum wheel," *Eur. J. Contr.*, Vol. 3, 1997, pp. 114-124.

7. Nam, M.-R., Hashimoto, T., and Ninomiya, K., "Control system design to cope with non-linearities of a magnetically suspended momentum wheel for satellites," *Proceedings of the 1st Int. Conf. on Non-linear Problems in Aviation and Aerospace*, Florida, USA, May, 1996, pp. 513-517.

8. Nam, M.-R., Hashimoto, T., and Ninomiya, K., "Combined application of H_∞ and sliding mode theories to attitude control of a satellite," *Proceedings of the 2nd Asian Contr. Conf.*, Seoul, Korea, July, 1997, pp. 827-830.

9. Trumper, D. L., Olson, S. M., and Subrahmanyan, P. K., "Linearizing control of magnetic suspension systems," *IEEE Trans. Contr. Syst. Technol.*, Vol. 5, No. 4, 1997, pp. 427-438.

10. Hong, S.-K., and Langari, R., "Robust fuzzy control of a magnetic bearing system subject to harmonic disturbances," *IEEE Trans. Contr. Syst. Technol.*, Vol. 8, No. 2, 2000, pp. 366-371.

11. Leon, S. J., *Linear Algebra with Applications*, Prentice-Hall, Singapore. 1995.

12. Bichler, U. J., "A low noise magnetic bearing wheel for space application," *Proceedings of the 2nd Int. Symp. Magn. Bearings*, Tokyo, Japan, July, 1990, pp. 1-8.

13. Herzog, R., Bühler, P., Gähler, C., and Larsonneur, R., "Unbalance compensation using generalized notch filters in the multivariable feedback of magnetic bearings," *IEEE Trans. Contr. Syst. Technol., V*ol. 4, No. 5, 1996, pp. 580-586.